

# RSC Advances



This is an *Accepted Manuscript*, which has been through the Royal Society of Chemistry peer review process and has been accepted for publication.

*Accepted Manuscripts* are published online shortly after acceptance, before technical editing, formatting and proof reading. Using this free service, authors can make their results available to the community, in citable form, before we publish the edited article. This *Accepted Manuscript* will be replaced by the edited, formatted and paginated article as soon as this is available.

You can find more information about *Accepted Manuscripts* in the [Information for Authors](#).

Please note that technical editing may introduce minor changes to the text and/or graphics, which may alter content. The journal's standard [Terms & Conditions](#) and the [Ethical guidelines](#) still apply. In no event shall the Royal Society of Chemistry be held responsible for any errors or omissions in this *Accepted Manuscript* or any consequences arising from the use of any information it contains.

## Charge Transfer or Biradicaloid Character: Assessing TD-DFT and SAC-CI for Squarylium Dye Derivatives

G. Krishna Chaitanya <sup>a,c,\*</sup>, Avinash L. Puyad <sup>a</sup>, K. Bhanuprakash <sup>b</sup>

<sup>a</sup> School of Chemical Sciences, S.R.T.M. University, Nanded-431 606, India

<sup>b</sup> Inorganic Chemistry Division, Indian Institute of Chemical Technology, Hyderabad, India.

<sup>c</sup> Present address: Materials Research Laboratory, University of Nova Gorica, Slovenia, SI 5000,

### Abstract

Keeping in view to suggest one more class of molecules in order to make a choice and assessment of exchange-correlation (XC) functionals, symmetrical squarylium dye (SQ) derivatives have been considered and Le Bahers's diagnostic indexes have been applied to study the electronic transition character of these molecular systems through TD-DFT and SAC-CI methods. Unlike calculated absorption using SAC-CI, the TD-DFT results are not matching with experimental absorption. However the diagnostic indexes obtained with TD-DFT and SAC-CI are apparently similar for all methods. This indicates that care should be taken while choosing XC functionals and assessing the nature of electronic transitions of a specific class of molecules. The centroids of charges associated with the density increase and depletion regions are localized on central C4 ring and carbonyl groups and with a small extension up to side aromatic substitution of the SQ dye derivative. Hence the electronic transition occurring in this class of molecules is confined mainly within the central part of molecule. This is in contrast to Donor-Acceptor-Donor type structure in which charge depletion region is expected at side aromatic substitution of the molecule. The small values of calculated transferred charge ( $q^{CT}$ ) upon excitation lend support to the theory that the electronic transition in this class of molecules is not CT excitation. This is in agreement with our earlier finding that biradicaloid character and orbital interactions are playing key role in their NIR absorption. Hence highly correlated, single reference and multi-determinant SAC-CI method is able to explain the nature of electronic excitations in these molecules rather than TD-DFT with various type of XC functionals.

## Introduction

The successful application of time-dependent density functional theory (TD-DFT) by standard generalized gradient approximations (GGA) and hybrid exchange-correlation (XC) functionals for the study of electronic excited states of the molecular systems has been well documented.<sup>1-4</sup> In particular, the local excitations (those involving minimal charge reorganization) are often accurately calculated within few tenths of electron Volts.<sup>5,6</sup> Recently, many studies have highlighted the shortcomings of TD-DFT at predicting excitations involving Rydberg energy states and perhaps in charge-transfer (CT) states. The asymptotic correction of the XC contribution to the Kohn-Sham equations is a remedy for excitations involving Rydberg states.<sup>7-10</sup> In case of CT excitations, the inadequate behaviour of traditional XC functional is attributed to incapability of understanding hole and electron. It is also deduced that this failure is due to insufficient long-range exchange effect in the exchange functionals.<sup>11</sup> Inclusion of fraction of non-local Hartree-Fock (HF) exchange has been suggested to overcome this shortcoming and several methodologies have been developed. In long range corrected (LC) hybrids HF exchange ratio increases with distance between two electrons hence better treatment of charge separated systems.<sup>11</sup> In the same way, Coulomb attenuated method (CAM), depends on additional three flexible parameters and incorporated in LC scheme has been suggested for several CT systems.<sup>12</sup> On the other hand, applications and validations of several Minnesota density functional methods have also been assessed recently for valence, Rydberg and CT based systems.<sup>13</sup>

Apart from the success of these new developments in XC functional, few important issues have to be noted from recent reports. The inclusion of long range HF exchange into TD-DFT affects the well known accuracy of local excitations which is a serious problem.<sup>14</sup> Li *et al* reported that Minnesota functionals are superior than LC functionals for CT excitations with intermediate spatial overlap of orbitals.<sup>15</sup> In spite of that, the potential of LC functionals for predicting the CT excitations has been greatly supported by several reports.<sup>16-22</sup> On the other hand, Nakano and co-workers highlighted that LC, CAM and Minnesota functionals are developed to minimize the errors between calculated and experimentally measured data only for several molecular sets.<sup>23</sup> Hence there is no assurance of accuracy of results obtained by these methods for a specific set of molecules.

These results indicate that there is a need of a diagnostic test for assessing the nature of electronic transitions obtained by TD-DFT and *ab-initio* methods. Several methodologies

have been reported recently which include geometrical descriptors and indexes based on molecular orbitals or electron densities involved in such electronic transitions.<sup>24-29</sup> Apart from limitations of these methods with respect to reliability, few methods have been extensively used as diagnostic tool for assessing TD-DFT results for local, CT and Rydberg kind of electronic transitions.<sup>24,26,30</sup> One among them based on overlap of molecular orbital moduli is  $\Lambda$ -index and has been successfully applied as diagnostic tool for different molecular systems.<sup>24,31-32</sup> Whenever the extent of orbital overlap is small, through space CT is thus expected and then the  $\Lambda$ -index values will be small enough. Large errors have been predicted for standard GGA and hybrid functionals where range-separated hybrids such as CAM-B3LYP are suggested. In contrary, this index cannot warn for CT kind of transitions while CT transitions with substantial overlap are correctly obtained by TD-DFT with large  $\Lambda$  values, for example 4-(N,N-dimethylamino)benzonitrile (DMABN).<sup>24,31-32</sup> As pointed out by authors, the problematic excitation where the electron is excited to a spatially extended orbital has not been explained by standard GGA functionals for systems with medium  $\Lambda$  values like triazenes.<sup>32</sup>

On the other hand, another sophisticated index has been proposed by Le Bahers *et al*, based on centroids of charge density depletion and charge density increment regions as a qualitative measure of CT associated with electronic excitation.<sup>26</sup> This density based descriptor has also been found application in studying the excited state evolution, excited state signatures and minimum energy reaction pathways [33-37]. The spatial distance between the two barycenters of density distributions as a measure of the CT excitation length is given as  $D^{\text{CT}}$ . For rod like donor-acceptor (D-A) systems, the half of these centroids axis along D-A direction is defined as H-index. The correlation between these two indexes has been suggested as a diagnostic tool for the performance of TD-DFT as well as warning sign of CT excitation. For  $H \geq D^{\text{CT}}$ , the substantial overlap between the centroids along this direction is observed. If  $H \leq D^{\text{CT}}$  then the overlap between centroids will be very weak and through space CT is seen. The difference between  $D^{\text{CT}}$  and H is given as  $t$ -index and has been suggested as diagnostic tool for TD-DFT results. If  $t > 1.6 \text{ \AA}$ , then such excitation seems to be potentially problematic transition for standard GGA and hybrid functionals. In such cases the range separated functionals are suggested to cure this problem.<sup>26</sup>

Even though, the validity of this method has been successfully tested with several D-A type of systems (unidirectional charge flow), the symmetrical systems like squarylium (SQ)

and croconate (CR) dye derivatives (scheme 1) have not been tried out for which the net flow of charge is negligible.<sup>38-40</sup> Conventionally, SQ dyes and CR dyes were known as D-A-D type of systems and believed that the donor (from the side substituent) and acceptor (central four-membered/ five-membered ring, respectively, and the carbonyl oxygens) abilities will influence their absorption spectrum.<sup>41-46</sup> In contrary, from our earlier calculations through high level *ab-initio* and density functional theory (DFT) calculations, the biradicaloid character (BRC) of these dyes has been unveiled and shown that the orbital interactions and C-C-C angle in the central ring of SQ/CR are playing a major role in their near infrared (NIR) absorption rather than D-A-D phenomenon.<sup>47-49</sup>

In the same way, the poor performance of LC and CAM functionals for the SQ and CR dye derivatives has been already reported by our group whereas the symmetry adapted cluster configuration interaction (SAC-CI) method correctly describes the electronic transitions in these BRC systems.<sup>50,51</sup> SAC-CI method has also been examined for the study of through-space CT excitation in comparison with TD-DFT methods.<sup>52-54</sup> Tawada et al. have found that LC-TD-DFT gives a correct intermolecular behavior of CT energy which is almost identical with the behavior of SAC-CI method.<sup>54</sup> The applicability and performance of TD-DFT with long-range corrected XC functionals along with SAC-CI method for rydberg and valence excited states have also been studied with benchmark set.<sup>55</sup> Also the correlation of chemically intuitive indexes for CT excitation based on SAC-CI and TD-DFT calculations on push-pull type of CT systems has been successfully described.<sup>56</sup>

From the above discussion, it is seen that the validation of Le Bahers's qualitative diagnostic tool has been done through unidirectional charge transfer systems and it also remains a scope for the study of understanding the electronic transition mechanism of symmetrical systems. On the other hand, the successful application of single reference and multi-determinant SAC-CI method is found not only for oxyallyl (OXA) substructured (scheme 1) and biradicaloid SQ and CR derivatives, but also for Rydberg, valence and CT systems. Hence there is a need for study of qualitative analysis and success of SAC-CI method for symmetrical SQ dye derivatives. Keeping this in view, fourteen SQ dye derivatives have been selected in this study to analyze the electronic transition mechanism by using TD-DFT, SAC-CI and Le Bahers's diagnostic tool. Also, this study has an important objective of suggesting one more class of molecules in order to make a choice and assessment of XC-functionals.

## Computational methodology

The results of the calculations reported in this work have been obtained using the Gaussian 09 ab initio/DFT quantum chemical simulation package.<sup>57</sup> Total fourteen SQ dyes shown in Fig. 1 are examined. The gas phase optimization of all the possible conformations of these dyes has been carried out using the hybrid density functional-B3LYP and Pople's split valence basis set with polarization and diffuse functions [6-311+G(d,p)] using the default integration grid and without symmetry constraints. The obtained minima are further confirmed by the frequency calculation at the same level. Only the lowest energy conformation is reported here.

The singlet geometries obtained at B3LYP level were subjected to TD-DFT and SAC/SAC-CI calculations to study the singlet-singlet transition. As there is a negligible difference between excitation energies obtained in gas phase and solvent media, only gas phase results have been given here for all molecules.<sup>47-51</sup> The hybrid XC functionals B3LYP and BHandHLYP, meta hybrid functionals M06-HF and M06-2X, dispersion corrected functional  $\omega$ B97XD and range corrected functionals LC- $\omega$ PBE and CAM-B3LYP have been used for TD-DFT calculations.<sup>6,12,58-65</sup> The SAC-CI is restricted to singles and doubles linked operators, while the higher order ones are treated through unlinked operators. All orbitals are considered in active space for SQ-1 whereas, active space of 150 to 200 orbitals is chosen with the window option due to the large size of all other molecules in SAC/SAC-CI calculation. The detailed methodology of SAC-CI is given elsewhere.<sup>66-71</sup> Four lowest excited states for each irreducible representation of each molecule are obtained.

In order to study the extent of CT or charge reorganization during the excitations, the qualitative index proposed by Le Bahers *et al* has been adopted here. The computed electronic wave functions obtained at ground and excited states are used to quantify the net charge transferred ( $q^{CT}$ ), CT length ( $D^{CT}$ ), variation in dipole moment ( $\mu^{CT}$ ), H-index and overlap between centroids of charge increased and charge depletion regions ( $C^+/C^-$ ) during the electronic excitation by using Multiwfn code.<sup>72</sup>

## Results and Discussion

The CT behavior can be determined by small spatial overlap of orbitals involved in the electron transition *i.e.* mainly by highest occupied molecular orbital (HOMO) and lowest unoccupied molecular orbital (LUMO) and associated dipole moment change. One of the best available examples studied with this index are prototype D-A-D type dyads where donor and acceptor are  $-NH_2$  and  $-NO_2$  respectively and significant CT is modulated through increasing number of conjugated phenyl rings as bridge in each dyad.<sup>26</sup> Based on number of phenyl rings between donor and acceptor groups they are represented as P<sub>n</sub> systems where n=1-4. The experimental absorption spectroscopy of these dyads shows that there is not much difference from P1 to P2 but the absorption decreases from P2 to P3 and P3 to P4 further.<sup>73</sup> It is expected that with increasing number of phenyl rings between donor and acceptor groups the extent of charge-separation should be varying and increasing the dipole moment change upon excitation. But, nothing more than the experimental absorption trend has been obtained with PBE0 and also even range-separated LC-PBE and CIS methods failed to describe the CT electronic excitation spectrum for these molecules.<sup>26</sup> On the other hand, results obtained with SAC-CI method correctly reproduced the effect of solvent polarization on the stabilization of the charge-separated state with respect to the donor-acceptor distance.<sup>56</sup>

In another report, TD-DFT study on triazene derivative has emphasized on influence of the increased fraction of exact, non-local exchange at long-range from GGA to hybrid and range separated hybrid functionals. Here in this case, the electron transition has moderate orbital overlap between HOMO and LUMO but still large errors reported for PBE and this problem is resolved by CAM-B3LYP.<sup>32</sup>

On the other hand, there are other studies where CT excitations are successfully explained by TD-DFT with standard hybrid functionals such as B3LYP and results are surprisingly accurate. An example is the calculation of absorption spectra of series of aromatic donor-acceptor systems of 4-(N,N-dimethylamino)benzonitrile (DMABN) for which the CT excitation is accurate to within a few tenths of an eV.<sup>74</sup> This surprising behavior has been reasoned out to the large overlap between the frontier orbitals which are directly involved in the excitation.<sup>24</sup> It has been characterized as CT excitation based on a large dipole moment change upon excitation, which does not imply a small occupied-virtual orbital overlap.<sup>75</sup>

So far, the different types of electronic excitations have been addressed with regard to small, medium and large overlap between electron donor and acceptor regions. The importance of dipole moment change upon excitations is discussed to assess their CT behavior. In this report we are presenting another class of molecules i.e. OXA substructure based SQ derivatives in which the extent of overlap between HOMO and LUMO is fairly large and were thought to be D-A-D type of molecules.<sup>41-46</sup>

In continuation of our previous reports concerning to the understanding of electronic structure of SQ dye derivatives, in this work the extent of charge separation and electronic transitions of fourteen molecules have been studied by Le Bahers's diagnostic indexes. The main difference among these molecules is the side electron rich aromatic groups such as phenyl, pyrylium, thiopyrylium, pyrrole, thiophene, indole, quinoline, benzoxazole and benzothiazole derivatives including simple  $-NH_2$  group. The calculated absorption wavelengths with various XC functionals by TD-DFT method and SAC-CI along with experimental absorption are given in table 1. It is seen from this table that the poor dependence of XC functions on the calculated absorption wave lengths indicates the cyanine like transitions for which TD-DFT is difficult to model them.<sup>86-89</sup> Apart from the limitations of TDDFT mentioned in the previous sections, electron transitions in cyanine derivatives remained as a puzzle. The inadequate treatment of correlation between ground and excited state with TDDFT is remained as a convincing explanation for its failure.<sup>86-89</sup> On the other hand, optical absorption and third-order polarizabilities of series of cyanine dyes have been obtained successfully by using dynamic correlated SAC-CI method.<sup>90</sup> The contribution of double excitations to the excited state wave function of both cyanine and OXA substructure dyes is another common feature of their electronic structure.<sup>47-51, 90</sup> The SAC-CI calculated wave function of all SQ dyes have been given in table 2. The transition from HOMO-LUMO single excitation has maximum CI coefficient of 0.94 where 0.92 has been reported in ref. 89 for cyanines along with less prominent double excitations in both cases those are actually missing at TDDFT level (supporting information).

However, except for SQ-1, none of the TD-DFT results *i.e.* hybrid XC functionals B3LYP and BhandHLYP, meta hybrid functionals M06-HF and M06-2X, dispersion corrected functional  $\omega$ B97XD and range corrected functional LC- $\omega$ PBE and CAM-B3LYP are in good agreement with experiment unlike with the case of SAC-CI which was reasoned out to the OXA substructure and BRC of these molecular systems.<sup>47-51</sup> In general, a molecule can be treated as biradicaloid if the singlet and triplet energy states separation is below 1eV.<sup>91</sup> Unlike

for all other molecules, SQ-1 has large HOMO-LUMO gap and singlet-triplet states energy splitting are found as 9.73eV and 2.26eV respectively.<sup>48</sup> Therefore SQ-1 cannot be categorized as biradicaloid molecule even though it has OXA substructure. Hence the TD-DFT method worked for this molecule.

The diagnostic index parameters have been calculated with both TD-DFT and SAC/SAC-CI method for all the molecules and are given in Fig.2a to Fig.2c for  $q^{CT}$ ,  $C^+/C^-$  and H-index respectively (the results including  $D^{CT}$ ,  $\mu^{CT}$  are given in Table S1 in supporting information). The current electronic densities for ground and excited states were obtained at SAC and SAC-CI levels respectively while SCF and lowest energy excited state densities were used for each XC functional. On comparison of the results from TD-DFT and SAC/SAC-CI methods some interesting features can be drawn. Even though experimental absorption wavelengths are not obtained with TD-DFT method, the diagnostic indexes are quite similar to the SAC/SAC-CI results.

As expected for symmetrical systems,  $D^{CT}$ , the distance between charge increment and depletion barycenters during electronic excitation are found nearly zero in all molecules, *i.e.* less than 0.010Å calculated by hybrid, meta-hybrid, range-separated hybrid, dispersion corrected functionals and highly correlated SAC/SAC-CI method (supporting information). For centrosymmetric D-A-D type of quadrupolar systems, equal amount of charge depletion from both side groups to the central acceptor group is anticipated. Indeed, due to their symmetry constraints, the average of charge depletion barycenteres (on side donor groups) coincides with the charge increment barycenter *i.e.* at central acceptor group. This gives the  $D^{CT}$  as zero for perfectly symmetrical systems and negligible values obtained in this study are due to small out of symmetry variations. This negligible  $D^{CT}$  values further leads to negligible  $\mu^{CT}$  values (supporting information).

To quantify the net CT quantity in these molecules,  $q^{CT}$  has been calculated and plotted in Fig. 2a. The net amount of charge transferred is negligible when compared to the standard CT type transitions and also not more than 0.5e obtained with irrespective of methodologies used for all the molecules. It is worth mentioning that if these SQ dyes are considered as D-A-D type of CT systems then CT from each donor group is even less than 0.25e to the central C4 ring. Thus, charge reorganization takes place instead of CT during the electronic excitation in these systems. It is also seen from Fig.2a that there is no correlation obtained with XC functional on net CT quantity in these systems. This clearly indicates that

care should be taken about the choice of XC functional while assessing the electronic structure of specific class of molecules. Correlation study of indexes obtained with different methodologies will not guarantee the accuracy of excitation energies obtained by them.<sup>26,56</sup>

In order to address this, the total charge depletion ( $C^-$ ), increment regions ( $C^+$ ) and variation of charge density upon excitation ( $\Delta\rho$ ) have been depicted in Fig. 3. The blue and cyan color regions corresponding to charge increment and charge decrement respectively. In contrary to the D-A-D phenomenon, both the charge increment and depletion regions are mainly centered around the central C4 ring. The difference in the donor ability of side aromatic groups is not represented in the charge depletion plots which is clear from simple -NH<sub>2</sub> groups to large benzoxazole/benzothiazole groups. From the last column of Fig.3, the variation of charge density between ground and excited states is mainly located on the central ring part with negligible contribution from electron rich side donor groups. This is again resembled from the maximum overlap of  $C^+$  and  $C^-$  regions which is shown in Fig. 2d. Irrespective of the methodology, the extent of overlap of  $C^+$  and  $C^-$  regions is not differed for all molecules except for only SQ-1 which is not considered as biradicaloid and TD-DFT is successful. This shows neither the side aromatic substitutions nor hetero atoms present in them are having any significant contribution in this electronic transition mechanism. Hence the NIR absorption of SQ dye derivatives is accompanied with charge reorganization in the central part of the molecule irrespective of the nature of donor strength of the side aromatic substituent.<sup>92</sup>

Another important index for rod like systems, H-index is defined to understand the extent of overlap between electron donating and electron accepting regions. From Fig. 2c, the large H-index values are resultant of confined overlap of  $C^+$  and  $C^-$  regions around central C4 ring and thus there is no charge separation existing in these molecules. The observed variations for H-index values among phenyl derivatives i.e. SQ-2, SQ-3, SQ-4, SQ-8 and SQ-10 are assigned for different substitutions on phenyl groups by which the charge stabilization at OXA substructure of central C4 ring takes place rather than affecting on CT behavior.<sup>47</sup> Similar observation is found in between pyrylium and thiopyrylium derivatives, and pyrrole and thiophene derivatives. This is in support to BRC of these molecules where orbital interaction between carbonyl oxygens and central C4 ring actually plays major role in their NIR absorption.<sup>47-51</sup>

All of these Le Bahers's diagnosing indexes are showing that there is no charge-separated state existing in SQ dye derivatives and there exists a perfect overlap of charge depletion and charge increment centroids. Moreover both the centroids have been localized at and around central C4 ring. These findings have significant correlation with the recent developments in experimental chemistry and materials sciences. New promising materials have been synthesized by substituting electron withdrawing groups at central C4 ring for variety of optical response applications.<sup>79,93-98</sup>

### Conclusions:

The extent of overlap between electron donor and acceptor regions is a key parameter to assign the nature of electronic transition. Based on this electronic transitions are assigned as local, CT and Rydberg types. In this study, another class of molecules *i.e.* OXA substructure based SQ dye derivatives have been studied which were thought to be D-A-D type of molecules but shown as biradicaloid species.

Le Bahers's diagnostic indexes have been used to study the electronic structure of these molecules through TD-DFT and SAC-CI methods. Even though the TD-DFT results are not matching with the experimental absorption, the diagnostic indexes are quite similar to the results obtained with SAC-CI. This clearly indicates that care should be taken while choosing XC functionals and assessing the nature of electronic transitions of a specific class of molecules. The centroids of charges associated to the density increase and depletion regions are localized on central C4 ring and carbonyl groups and with a small extension up to side aromatic substitution of the SQ dye derivative. Hence the electronic transition occurring in this class of molecules is confined mainly within the central part of molecule. This is in contrast to the experimentalist hypothesis of D-A-D type structure in which charge depletion region is expected at side aromatic substitution of the molecule. The calculated transferred charge ( $q^{CT}$ ) upon excitation is less than 0.25e with respect to each side aromatic donor group which is supporting that the electronic transition in this class of molecules is not CT excitation. This is in agreement with our earlier finding about BRC and orbital interactions are playing key role in their NIR absorption. Hence highly correlated, single reference and multi-determinant SAC-CI method is able to explain the nature of excitations in these molecules rather than TD-DFT with various type of XC functionals.

This observation helps experimentalists in understanding the molecular structure of symmetrical SQ dye derivatives for further design and development of novel molecules in

materials chemistry. To support this, the tuning of electronic absorption spectrum of SQ derivatives by incorporating electron withdrawing groups at electron rich central C4 ring has become a promising design principle for novel materials recently.<sup>79,93-98</sup>

### **Acknowledgements**

GKC thanks DST, New Delhi for financial assistance (NO.SR/FT/CS-133/2010). G09 software has been procured under the DST-FIST Scheme (Sanction No. FS/FST/PSI-018/2009). Authors acknowledge Dr. Tangui Le Bahers, Laboratoire de Chimie Ens de Lyon, France for useful discussions. Financial assistance through NWP0054 is acknowledged.

## References

1. E. Runge and E. K. U. Gross, *Phys. Rev. Lett.*, 1984, **52**, 997–1000
2. E. K. U. Gross, C. A. Ullrich and U. J. Gossmann, in *Density Functional Theory*, ed. E. K. U. Gross and R. M. Dreizler, Plenum, New York, 1994, pp. 149–171
3. M. E. Casida, in *Recent Advances in Density Functional Methods, Part I*, ed. D. P. Chong, World Scientific, Singapore, 1995, pp. 155–192
4. M. A. L. Marques and E. K. U. Gross, *Annu. Rev. Phys. Chem.*, 2004, **55**, 427–455
5. J. P. Perdew, K. Burke and M. Ernzerhof, *Phys. Rev. Lett.*, 1996, **77**, 3865–3868
6. A. D. Becke, *J. Chem. Phys.*, 1993, **98**, 5648–5652
7. D. J. Tozer and N. C. Handy, *J. Chem. Phys.*, 1998, **109**, 10180
8. M. E. Casida, K. C. Casida, and D. R. Salahub, *Int. J. Quantum Chem.*, 1998, **70**, 933
9. M. J. Allen and D. J. Tozer, *J. Chem. Phys.*, 2000, **113**, 5185
10. M. Grüning, O. V. Gritsenko, S. J. A. van Gisbergen, and E. J. Baerends, *J. Chem. Phys.*, 2001, **114**, 652
11. H. Iikura, T. Tsuneda, T. Yanai, and K. Hirao, *J. Chem. Phys.*, 2001, **115**, 3540
12. T. Yanai, D.P. Tew and N.C. Handy, *Chem. Phys. Lett.*, 2004, **393**, 51–57
13. Y. Zhao and D. G. Truhlar, *Chem. Phys. Lett.*, 2011, **502**, 1–13
14. D. Jacquemin, E.A. Perpète, G.E. Scuseria, I. Ciofini and C. Adamo, *J. Chem. Theory Comput.* 2008, **4**, 123
15. R. Li, J. Zheng and D.G. Truhlar, *Phys. Chem. Chem. Phys.*, 2010, **12**, 12697
16. Y. Xue, L. An, Y. Zheng, L. Zhang, X. Gong, Y. Qian and Y. Liu, *Comput. Theor. Chem.*, 2012, **981**, 90–99
17. F. B. Anne, F. D. Purpan and D. Jacquemin, *Chem. Phys. Lett.*, 2013, **581**, 52–56
18. P. J. Aittala, O. Cramariuc and T. I. Hukka, *Chem. Phys. Lett.*, 2011, **501**, 226–231
19. A. J. Garza, G. E. Scuseria, S. B. Khan and A. M. Asiri, *Chem. Phys. Lett.*, 2013, **575**, 122–125
20. X. Liu, X. Zhang, Y. Hou, F. Teng and Z. Lou, *Chem. Phys.*, 2011, **381**, 100–104
21. J. J. Eriksen, S. P.A. Sauer, K. V. Mikkelsen, O. Christiansen, H. J. A. Jensen and J. Kongsted, *Mol. Phys.*, 2013, **111**, 1235–1248
22. G. Garci, C. Adamo and I. Ciofini, *Phys. Chem. Chem. Phys.*, 2013, **15**, 20210
23. K. Okuno, Y. Shigeta, R. Kishi, H. Miyasaka and M. Nakano, *J. Photochem. Photobiol., A*, 2012, **235**, 29–34
24. M. J. G. Peach, P. Benfield, T. Helgaker, and D. J. Tozer, *J. Chem. Phys.* 2008, **128**,

044118

25. T. Ziegler, M. Seth, M. Krykunov and J. Autschbach, *J. Chem. Phys.* 2008, **129**, 184114
26. T. L. Bahers, C. Adamo and I. Ciofini, *J. Chem. Theory Comput.* 2011, **7**, 2498–2506
27. H. Nitta and I. Kawata, *Chem. Phys.* 2012, **405**, 93–99
28. M. J. Bedard-Hearn, F. Sterpone and P. J. Rossky, *J. Phys. Chem. A* 2010, **114**, 7661–7670
29. F. Plasser and H. Lischka, *J. Chem. Theory Comput.* 2012, **8**, 2777–2789
30. C. A. Guido, P. Cortona, B. Mennucci and C. Adamo *J. Chem. Theory Comput.* 2013, **9**, 3118–3126
31. M. J. G. Peach and D. J. Tozer, *J. Mol. Struct.: THEOCHEM*, 2009, **914**, 110–114
32. M. J. G. Peach, C. R. L. Sueur, K. Ruud, M. Guillaume and D. J. Tozer, *Phys. Chem. Chem. Phys.* 2009, **11**, 4465–4470
33. M. Savarese, P.A. Netti, N. Rega, C. Adamo and I. Ciofini, *Phys. Chem. Chem. Phys.*, 2014, **16**, 8661.
34. S. Chibani, A. Charaf-Eddin, B. Mennucci, B. Le Guennic, and D. Jacquemin, *J. Chem. Theory Comput.* 2014, **10**, 805–815.
35. M. Savarese, P.A. Netti, C. Adamo, N. Rega and I. Ciofini, *J. Phys. Chem. B*, 2013, **117**, 16165.
36. D. Jacquemin, T. L. Bahers, C. Adamo and I. Ciofini, *Phys. Chem. Chem. Phys.*, 2012, **14**, 5383.
37. I. Ciofini, T. L. Bahers, C. Adamo, F. Odobel and D. Jacquemin, *J. Phys. Chem. C*, 2012, **116**, 11946.
38. H. Li, J. Zhang, Y. Wu, J. Jin, Y. Duan, Z. Su and Y. Geng, *Dyes Pigm.*, 2014, **108**, 106–114
39. S. D. Sousa, L. Ducasse, B. Kauffmann, T. Toupance, and C. Olivier, *Chem. Eur. J.*, 2014, **20**, 7017–7024
40. Y. Nicolas, F. Allama, M. Lepeltier, J. Massin, F. Castet, L. Ducasse, L. Hirsch, Z. Boubegtiten, G. Jonusauskas, C. Olivier, and T. Toupance, *Chem. Eur. J.*, 2014, **20**, 3678–3688
41. H. Langhals, *Angew. Chem. Int. Ed.* 2003, **42**, 4286–4288
42. H. Meier and U. Dullweber, *J. Org. Chem.*, 1997, **62**, 4821–4826
43. H. Meier and U. Dullweber, *Tetrahedron Lett.*, 1996, **37**, 1191–1194

44. H. Meier, R. Petermann and J. Gerold, *Chem. Comm.*, 1999, 977–978
45. K. Y. Law, *J. Phys. Chem.*, 1987, **91**, 5184–5193
46. R. W. Bigelow and H. J. Freund, *Chem. Phys.*, 1986, **107**, 159–174
47. Ch. Prabhakar, G. Krishna Chaitanya, Sanyasi Sitha, K. Bhanuprakash and V. J. Rao, *J. Phys. Chem. A*, 2005, **109**, 2614-2622
48. Ch. Prabhakar, K. Yesudas, G. Krishna Chaitanya, Sanyasi Sitha, K. Bhanuprakash and V. J. Rao, *J. Phys. Chem. A*, 2005, **109**, 8604-8616
49. A. L. Puyad, Ch. Prabhakar, K. Yesudas, K. Bhanuprakash and V. J. Rao, *J. Mol. Struct. :THEOCHEM*, 2009, **904**, 1–6
50. A. L. Puyad, G. Krishna Chaitanya A. Thomas, M. Paramasivam and K. Bhanuprakash, *J. Phys. Org. Chem.*, 2013, **26**, 37–46
51. A. L. Puyad, G. Krishna Chaitanya, Ch. Prabhakar and K. Bhanuprakash, *J Mol Model*, 2013, **19**, 275–287
52. H. Nakatsuji, J. Hasegawa and K. Ohkawa, *Chem. Phys. Lett.*, 1998, **296**, 499
53. M. Ehara, J. Hasegawa and H. Nakatsuji, In *Theory and Applications of Computational Chemistry: The First 40 Years, A Volume of Technical and Historical Perspectives*, Ed C. E. Dykstra, G. Frenking, K. S. Kim and G. E. Scuseria, Elsevier: Oxford, 2005, pp. 1099–1141
54. Y. Tawada, T. Tsuneda, S. Yanagisawa, T. Yanai and K. Hirao, *J. Chem. Phys.* 2004, **120**, 8425
55. M. Alipour, *J. Phys. Chem. A*, 2014, **118**, 1741–1747
56. M. Ehara, R. Fukuda, C. Adamo and I. Ciofini, *J. Comput. Chem.* 2013, **34**, 2498–2501
57. Gaussian 09, Revision C.01, M. J. Frisch, G. W. Trucks, H. B. Schlegel, G. E. Scuseria, M. A. Robb, J. R. Cheeseman, G. Scalmani, V. Barone, B. Mennucci, G. A. Petersson, H. Nakatsuji, M. Caricato, X. Li, H. P. Hratchian, A. F. Izmaylov, J. Bloino, G. Zheng, J. L. Sonnenberg, M. Hada, M. Ehara, K. Toyota, R. Fukuda, J. Hasegawa, M. Ishida, T. Nakajima, Y. Honda, O. Kitao, H. Nakai, T. Vreven, J. A. Montgomery, Jr., J. E. Peralta, F. Ogliaro, M. Bearpark, J. J. Heyd, E. Brothers, K. N. Kudin, V. N. Staroverov, T. Keith, R. Kobayashi, J. Normand, K. Raghavachari, A. Rendell, J. C. Burant, S. S. Iyengar, J. Tomasi, M. Cossi, N. Rega, J. M. Millam, M. Klene, J. E. Knox, J. B. Cross, V. Bakken, C. Adamo, J. Jaramillo, R. Gomperts, R. E. Stratmann, O. Yazyev, A. J. Austin, R. Cammi, C. Pomelli, J. W. Ochterski, R. L. Martin, K. Morokuma, V. G. Zakrzewski, G. A. Voth, P. Salvador, J. J. Dannenberg, S. Dapprich,

- A. D. Daniels, O. Farkas, J. B. Foresman, J. V. Ortiz, J. Cioslowski, and D. J. Fox, Gaussian, Inc., Wallingford CT, 2010.
58. A. D. Becke, *J. Chem. Phys.*, 1993, **98**, 1372-77
59. Y. Zhao and D. G. Truhlar, *J. Phys. Chem.*, 2006, **110**, 5121-29
60. Y. Zhao and D. G. Truhlar, *J. Phys. Chem. A*, 2006, **110**, 13126-30
61. Y. Zhao and D. G. Truhlar, *Theor. Chem. Acc.*, 2008, **120**, 215-41
62. J.-D. Chai and M. Head-Gordon, *Phys. Chem. Chem. Phys.*, 2008, **10**, 6615-20
63. O. A. Vydrov and G. E. Scuseria, *J. Chem. Phys.*, 2006, **125**, 234109
64. O. A. Vydrov, J. Heyd, A. Krukau, and G. E. Scuseria, *J. Chem. Phys.*, 2006, **125**, 074106
65. O. A. Vydrov, G. E. Scuseria, and J. P. Perdew, *J. Chem. Phys.*, 2007, **126**, 154109
66. T. Nakajima and H. Nakatsuji, *Chem. Phys. Lett.* 1997, **280**, 79-84
67. J. Wan, M. Ehara, M. Hada and H. Nakatsuji, *J. Chem. Phys.* 2000, **113**, 5245-5252
68. T. Nakajima and H. Nakatsuji, *Chem. Phys. Lett.* 1999, **300**, 1-8
69. J. Wan, M. Hada, M. Ehara and H. Nakatsuji, *J. Chem. Phys.* 2001, **114**, 842-850
70. H. Nakatsuji, *ACH-Models Chem.*, 1992, **129**, 719-776
71. H. Nakatsuji, in *Computational Chemistry Reviews of Current Trends, Vol. 2*, Ed: J. Leszczynski, World Scientific, Singapore, 1997
72. T. Lu and F. Chen, *J. Comp. Chem.* 2012, **33**, 580-592
73. R. W. H. Berry, P. Brocklehurst and A. Burawoy, *Tetrahedron* 1960, **10**, 109-117
74. C. Jamorski, J. B. Foresman, C. Thilgen and H.-P. Luthi, *J. Chem. Phys.*, 2002, **116**, 8761-8771
75. C. Bulliard, M. Allan, G. Wirtz, E. Haselbach, K. Zachariasse, N. Detzer and S. Grimme, *J. Phys. Chem. A*, 1999, **103**, 7766-7772
76. E. W. Neuse and B. R. Green *J. Am. Chem. Soc.*, 1975, **97** (14), 3987-3991
77. H. Meier, R. Petermann and J. Gerold, *Chem. Commun.*, 1999, 977-978
78. D. G. Farnum, B. Webster and A. D. Wolf *Tetrahedron Lett* 1968, **9(48)**, 1968, 5003-5006
79. M. R. Detty and B. Henne *Heterocycles* 1993, **35(2)**, 1149-1156
80. A. Treibs, and K. Jacob *Angew. Chem. Int. Ed. Engl.*, 1965, **4**, 694
81. D. Keil, H. Hartmann and T. Moschny *Dyes and Pigments*, 1991, **17(1)**, 19-27
82. A. L. Tatarets, I. A. Fedyunyaeva, E. Terpetschnig and L. D. Patsenker *Dyes and Pigments*, 2005, **64(2)**, 125-134

83. K. Jyothish, K. T. Arun, and D. Ramaiah *Org. Lett.*, 2004, **6** (22), 3965–3968
84. V. V. Kurdyukov<sup>1</sup> and A. I. Tolmachev *Chem Heterocyclic Comp*, 2009, **45**(10), 1283–1284
85. U. Mayerhöffer, K. Deing, K. Groß, H. Braunschweig, K. Meerholz, F. Würthner, *Angew. Chem. Int. Ed.* 2009, 48, 8776–8779
86. A. D. Laurent and D. Jacquemin *Int. J. Quantum Chem.* 2013, **113**, 2019–2039
87. B. Moore II and J. Autschbach *J. Chem. Theory Comput.* 2013, **9**, 4991–5003
88. H. Zhekova, M. Krykunov, J. Autschbach, and T. Ziegler *J. Chem. Theory Comput.* 2014, **10**, 3299–3307
89. D. Jacquemin, E. A. Perpète, G. Scalmani, M. J. Frisch, R. Kobayashi and C. Adamo, *J. Chem. Phys.* 2007, 126, 144105.
90. K. Yesudas, *Phys. Chem. Chem. Phys.*, 2013, **15**, 19465
91. J. Wirz, *Pure Appl. Chem.* 1984, 56, 1289 – 1300
92. J. Fabian and R. Peichert *J. Phys. Org. Chem.* 2010, **23**, 1137–1145
93. L. Beverina, R. Ruffo, C. Maria Mari, G. A. Pagani, M. Sassi, F. De Angelis, S. Fantacci, J.-H. Yum, M. Gratzel, Md. K. Nazeeruddin, *ChemSusChem* 2009, 2, 621–624
94. A. L. Tatarsky, I. A. Fedyunyaeva, E. Terpetschnig and L. D. Patsenker, *Dyes Pigm.*, 2005, **64**, 125–134
95. Y. Xu, M. J. Panzner, X. Li, W. J. Youngs and Y. Pang, *Chem. Commun.*, 2010, **46**, 4073–4075
96. K. D. Volkova, V. B. Kovalska, M. Yu. Losytskyy, A. Bento, L. V. Reis, P. F. Santos, P. Almeida and S. M. Yarmoluk, *J. Fluoresc.*, 2008, **18**, 877–882
97. L. Beverina and P. Salice, *Eur. J. Org. Chem.*, 2010, 1207–1215
98. L. Beverina, R. Ruffo, M. M. Salamone, E. Ronchi, M. Binda, D. Natali and M. Sampietro, *J. Mater. Chem.*, 2012, **22**, 6704–6710

Scheme 1: Schematic representation of oxyallyl (OXA) substructure, squarylium (SQ) and croconate (CR) dye derivatives.

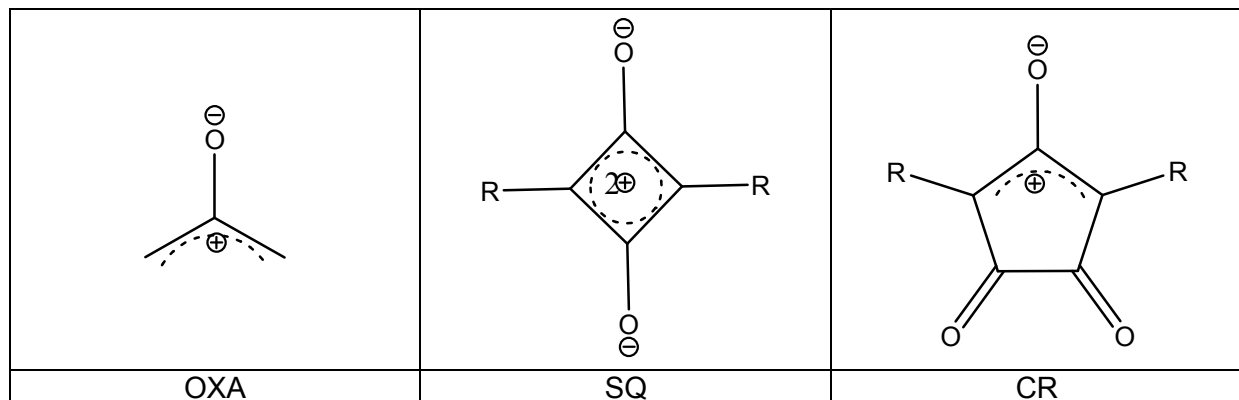


Table 1: Experimental and calculated absorption maxima (in nm) with TD-DFT and SAC-CI methodologies for all molecules.

Molecule	Experimental	SAC-CI	B3LYP	BHandHLYP	CAM-B3LYP	M06-HF	M06-2X	$\omega$ B97XD	LC- $\omega$ PBE
SQ-1	285 <sup>a</sup>	293	298	278	292	285	285	293	291
SQ-2	627 <sup>b</sup>	621	519	484	505	502	503	507	505
SQ-3	636 <sup>b</sup>	643	513	480	505	512	504	505	509
SQ-4	656 <sup>c</sup>	650	503	471	495	510	496	495	501
SQ-5	630 <sup>b</sup>	633	534	494	519	514	515	520	518
SQ-6	540 <sup>d</sup>	532	497	460	482	467	476	484	480
SQ-7	713 <sup>e</sup>	721	583	558	583	611	580	587	597
SQ-8	804 <sup>e</sup>	799	638	618	646	689	642	653	666
SQ-9	565 <sup>f</sup>	562	478	467	483	494	478	486	496
SQ-10	654 <sup>g</sup>	662	542	516	536	553	534	539	548
SQ-11	635 <sup>h</sup>	637	541	511	533	552	534	534	540
SQ-12	732 <sup>i</sup>	734	631	579	601	607	602	601	601
SQ-13	586 <sup>j</sup>	580	513	481	503	517	502	503	510
SQ-14	685 <sup>k</sup>	682	549	522	545	567	545	547	556

<sup>a</sup> ref. 76. <sup>b</sup> ref. 45. <sup>c</sup> ref. 77. <sup>d</sup> ref. 78. <sup>e</sup> ref. 79. <sup>f</sup> ref. 80. <sup>g</sup> ref. 81. <sup>h</sup> ref. 82. <sup>i</sup> ref. 83. <sup>j</sup> ref. 84. <sup>k</sup> ref. 85.

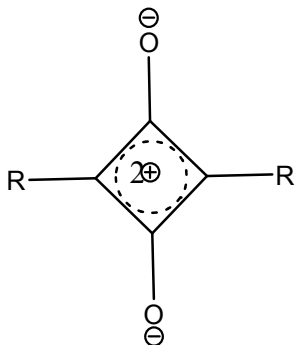
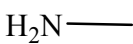
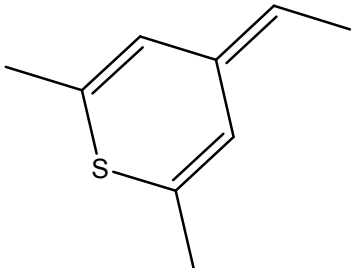
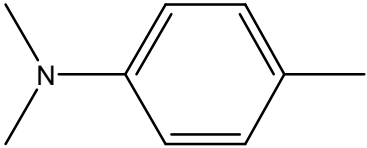
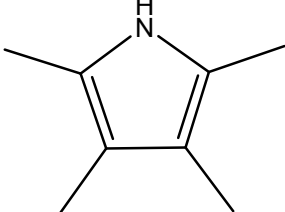
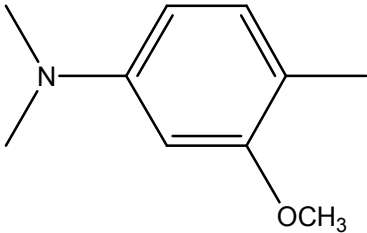
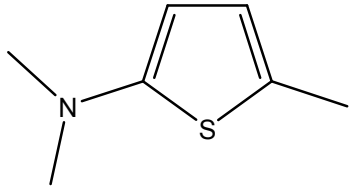
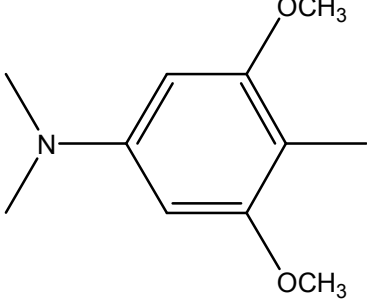
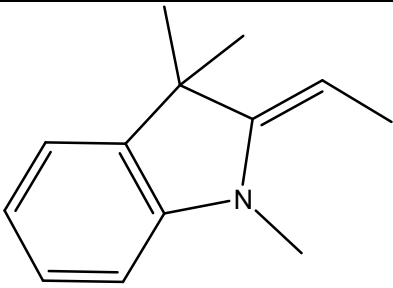
Table 2: Calculated absorption maxima ( $\lambda_{\max}$  in nm), oscillator strength ( $f$ ) and CI-wave function obtained at SAC-CI/6-311G(d,p) level (CI coefficient > 0.05 are reported here; H and L corresponds to HOMO and LUMO respectively).

Molecule	$\lambda_{\max}$	$f$	CI-wave function
SQ-1	293	0.355	-0.936(H→L)-0.104(H-7→L)+0.102(H-3→L)+0.067 (H-1→L+6)-0.066(H-1→L+4)+0.059(H-1→L+11)-0.177(H→L+8, H→L)-0.138(H→L+3, H-4→L)+0.074(H-3→L, H-5→L)+0.063(H-5→L, H-7→L)+0.061(H→L, H-4→L+3)-0.054(H→L+8, H-3→L)-0.053(H-3→L+3, H-4→L)
SQ-2	621	1.301	-0.939(H→L)+0.111(H-1→L+3)-0.063(H-21→L)-0.058(H-7→L)-0.112(H→L, H-1→L)-0.079(H→L+3, H→L)-0.072(H→L+11, H-1→L)+0.067(H→L+11, H-8→L)-0.065(H-1→L, H-2→L)+0.056(H→L+3, H-2→L)+0.053(H→L+10, H-10→L)-0.052(H→L+18, H-3→L)+0.050(H→L+2, H-4→L)
SQ-3	643	1.255	-0.937(H→L)-0.071(H-3→L+1)+0.062(H-1→L+1)+0.055(H-4→L)+0.050(H-2→L)+0.120(H→L, H-3→L)+0.088(H→L, H-1→L)-0.072(H→L+11, H-3→L)-0.070(H→L+11, H-6→L)+0.064(H→L+1, H-4→L)-0.062(H→L+1, H→L)-0.059(H→L, H-6→L)+0.056(H→L+28, H-4→L)
SQ-4	650	1.258	0.941(H→L)-0.104(H-3→L+2)+0.136(H→L, H-3→L)+0.093(H→L, H-6→L)+0.089(H→L+11, H-6→L)-0.066(H→L+2, H-4→L)+0.062(H→L+2, H→L)+0.061(H→L+11, H-3→L)+0.052(H→L+41, H-7→L)
SQ-5	721	1.230	0.940(H→L)-0.096(H-1→L+1)+0.189(H→L+1, H→L)+0.092(H→L+8, H-1→L)-0.060(H→L+5, H-1→L)-0.057(H-1→L, H-3→L)+0.057(H→L+34, H-3→L)+0.054(H→L+1, H-7→L)-0.053(H→L+11, H-1→L)
SQ-6	799	1.415	0.939(H→L)+0.103(H-1→L+1)+0.194(H→L+1, H→L)-0.104(H→L+8, H-1→L)+0.063(H→L+8, H-8→L)-0.060(H-1→L, H-2→L)-0.060(H→L+1, H-7→L)-0.056(H→L, H-1→L)-0.050(H→L+39, H-2→L)

SQ-7	682	1.390	$0.941(H \rightarrow L) + 0.077(H-1 \rightarrow L+3) - 0.062(H-1 \rightarrow L+9) - 0.059(H-1 \rightarrow L+1) - 0.053(H-25 \rightarrow L) - 0.109(H \rightarrow L+9, H \rightarrow L) - 0.091(H \rightarrow L, H-1 \rightarrow L) - 0.085(H \rightarrow L+3, H \rightarrow L) + 0.069(H \rightarrow L+27, H-6 \rightarrow L) + 0.061(H \rightarrow L+9, H-2 \rightarrow L) - 0.057(H \rightarrow L+52, H-7 \rightarrow L) - 0.051(H \rightarrow L, H-2 \rightarrow L)$
SQ-8	633	1.199	$0.941(H \rightarrow L) + 0.083(H-1 \rightarrow L+1) + 0.071(H-19 \rightarrow L) + 0.101(H \rightarrow L, H-1 \rightarrow L) - 0.072(H \rightarrow L+11, H-1 \rightarrow L) - 0.071(H \rightarrow L+1, H \rightarrow L) + 0.069(H-1 \rightarrow L, H-2 \rightarrow L) - 0.060(H \rightarrow L+8, H-9 \rightarrow L) + 0.059(H \rightarrow L+11, H-8 \rightarrow L) + 0.057(H \rightarrow L+30, H-2 \rightarrow L) + 0.051(H-2 \rightarrow L+8, H-9 \rightarrow L)$
SQ-9	637	1.242	$0.942(H \rightarrow L) + 0.088(H-1 \rightarrow L+3) + 0.059(H-29 \rightarrow L) - 0.099(H \rightarrow L+10, H \rightarrow L) - 0.097(H \rightarrow L, H-1 \rightarrow L) + 0.080(H \rightarrow L+3, H \rightarrow L) + 0.069(H \rightarrow L, H-6 \rightarrow L) - 0.059(H \rightarrow L+31, H-6 \rightarrow L) - 0.056(H \rightarrow L+10, H-2 \rightarrow L) + 0.052(H \rightarrow L+25, H-6 \rightarrow L)$
SQ-10	532	1.050	$-0.941(H \rightarrow L) - 0.087(H-20 \rightarrow L) - 0.067(H-5 \rightarrow L) - 0.050(H-7 \rightarrow L) + 0.079(H \rightarrow L+6, H-11 \rightarrow L) + 0.079(H \rightarrow L+1, H \rightarrow L) + 0.074(H \rightarrow L, H-1 \rightarrow L) + 0.068(H \rightarrow L+3, H \rightarrow L) + 0.066(H \rightarrow L+9, H-1 \rightarrow L) + 0.065(H-5 \rightarrow L+6, H-11 \rightarrow L) - 0.062(H \rightarrow L+31, H-5 \rightarrow L) - 0.061(H-1 \rightarrow L, H-5 \rightarrow L) - 0.058(H \rightarrow L+31, H \rightarrow L) + 0.056(H \rightarrow L+22, H-5 \rightarrow L) + 0.051(H-22, H \rightarrow L)$
SQ-11	562	1.233	$0.940(H \rightarrow L) + 0.067(H-1 \rightarrow L+3) + 0.065(H-2 \rightarrow L) + 0.130(H \rightarrow L, H-1 \rightarrow L) + 0.114(H \rightarrow L, H-3 \rightarrow L) + 0.093(H \rightarrow L+3, H \rightarrow L) - 0.072(H \rightarrow L+19, H-3 \rightarrow L) - 0.060(H-3 \rightarrow L, H-5 \rightarrow L) + 0.058(H \rightarrow L+36, H-5 \rightarrow L)$
SQ-12	734	1.452	$-0.935(H \rightarrow L) - 0.099(H-1 \rightarrow L+1) - 0.158(H \rightarrow L+1, H \rightarrow L) + 0.113(H \rightarrow L+7, H \rightarrow L) - 0.074(H \rightarrow L+2, H-1 \rightarrow L) + 0.055(H \rightarrow L+15, H-6 \rightarrow L) + 0.051(H \rightarrow L+2, H-3 \rightarrow L)$
SQ-13	662	1.220	$-0.935(H \rightarrow L) - 0.102(H \rightarrow L+1) - 0.068(H-5 \rightarrow L) - 0.062(H-2 \rightarrow L) - 0.053(H-21 \rightarrow L) - 0.124(H \rightarrow L+1, H \rightarrow L) + 0.108(H \rightarrow L, H-1 \rightarrow L) + 0.072(H \rightarrow L+6, H-1 \rightarrow L) + 0.070(H-1 \rightarrow L, H-2 \rightarrow L) + 0.056(H \rightarrow L+40, H-2 \rightarrow L)$

SQ-14	580	1.365	$0.944(H \rightarrow L) + 0.094(H-1 \rightarrow L+1) + 0.060(H-21 \rightarrow L) - 0.093(H \rightarrow L+10, H \rightarrow L) + 0.093(H \rightarrow L, H-1 \rightarrow L) + 0.090(H \rightarrow L+21, H-7 \rightarrow L) + 0.076(H \rightarrow L+12, H \rightarrow L) - 0.069(H \rightarrow L+1, H \rightarrow L) + 0.062(H \rightarrow L, H-7 \rightarrow L)$
-------	-----	-------	--

Figure 1: Molecular structures of SQ derivatives studied.

			
SQ-1		SQ-8	
SQ-2		SQ-9	
SQ-3		SQ-10	
SQ-4		SQ-11	

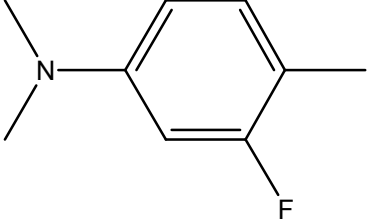
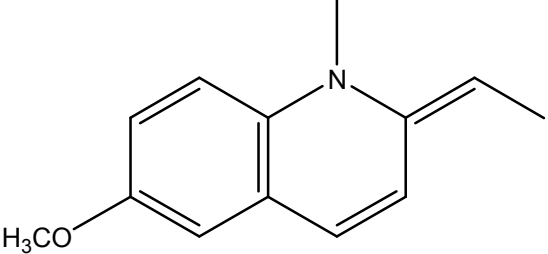
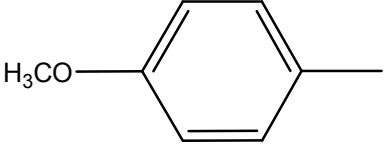
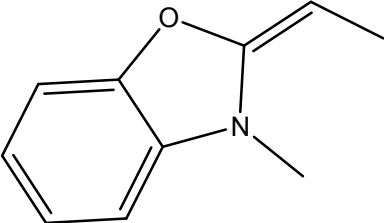
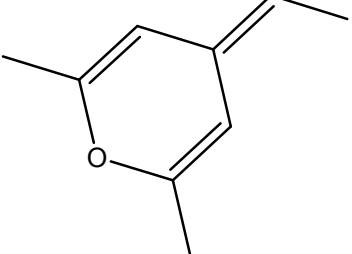
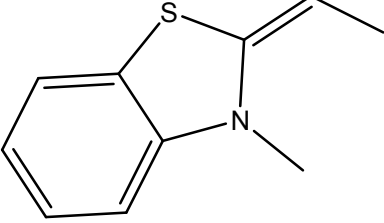
SQ-5		SQ-12	
SQ-6		SQ-13	
SQ-7		SQ-14	

Figure 2a: Net amount of charge transfer ( $q^{CT}$ ) for all molecules obtained at TD-DFT and SAC-CI levels.

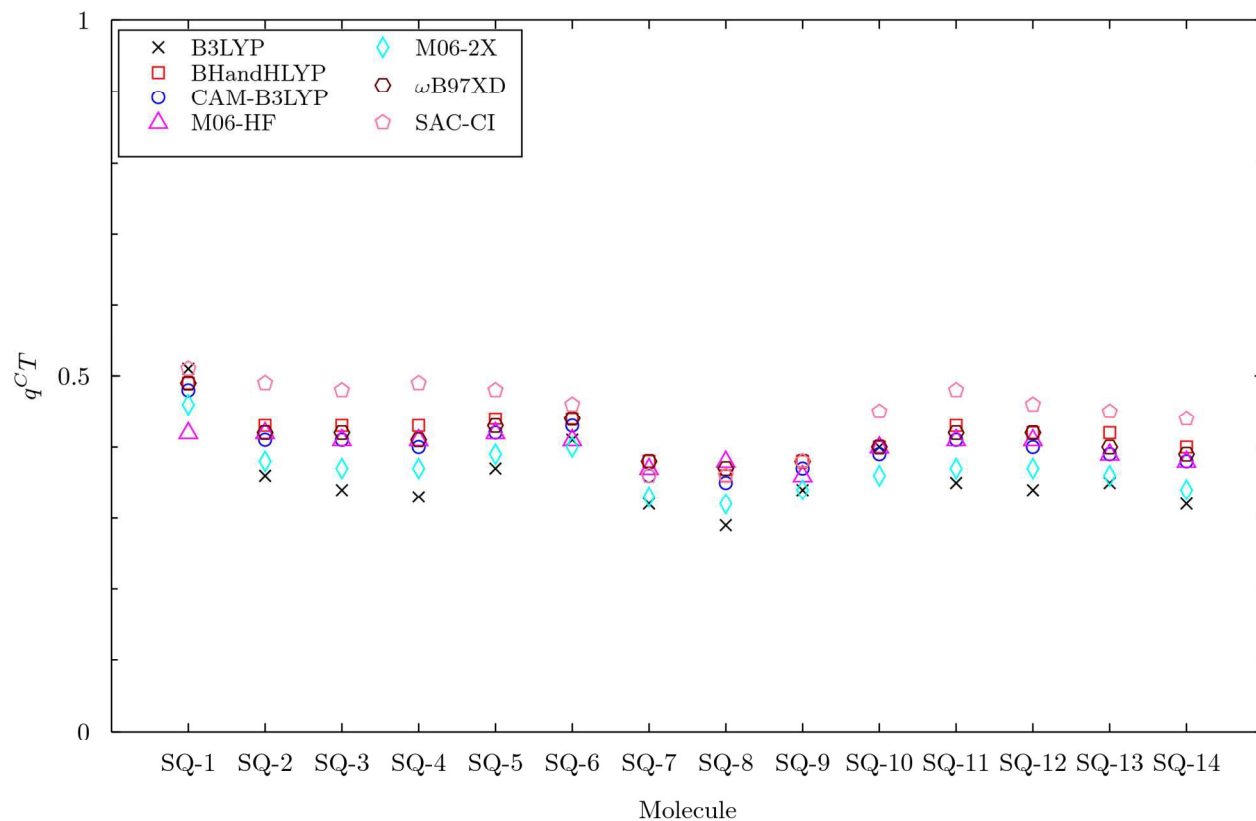


Figure 2b: Ratio of charge increment and charge depletion barycenters ( $C^+/C^-$ ) for all molecules obtained at TD-DFT and SAC-CI levels.

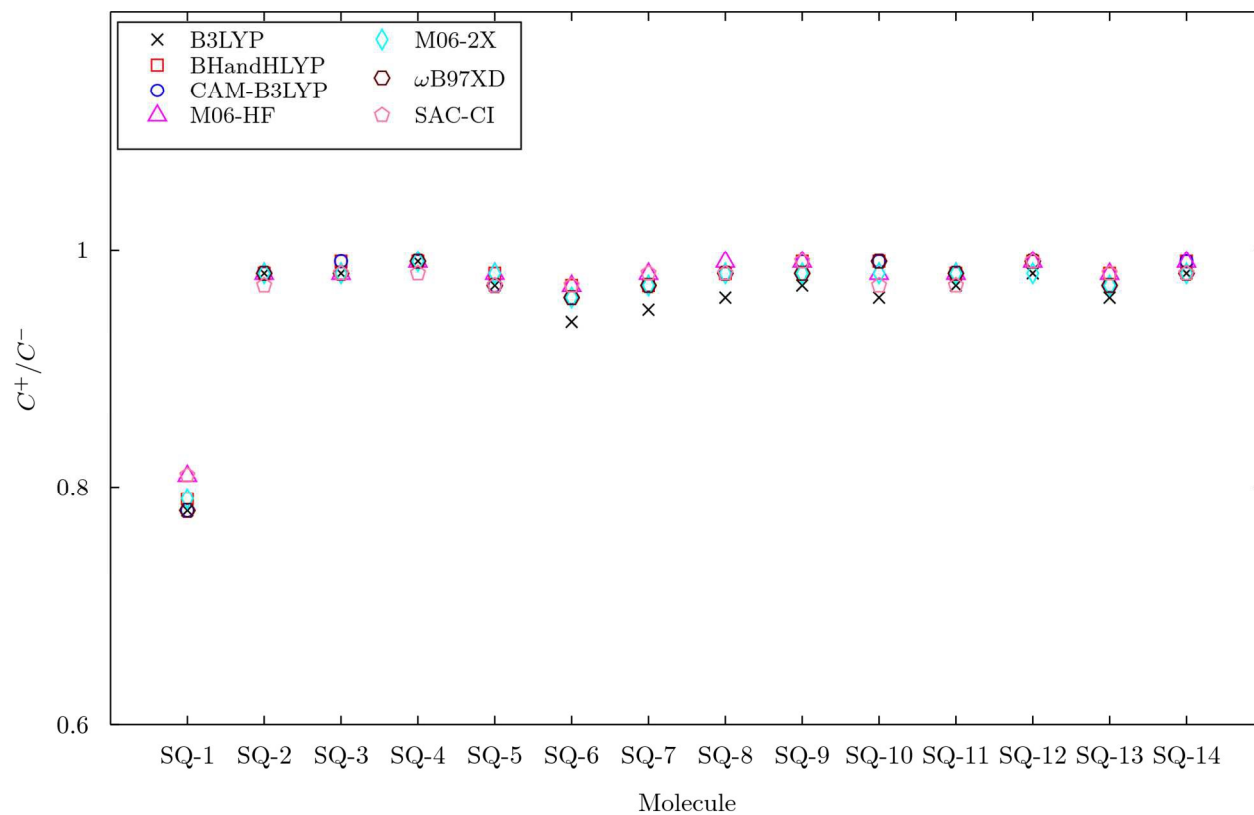


Figure 2c: H-index for all molecules obtained at TD-DFT and SAC-CI levels.

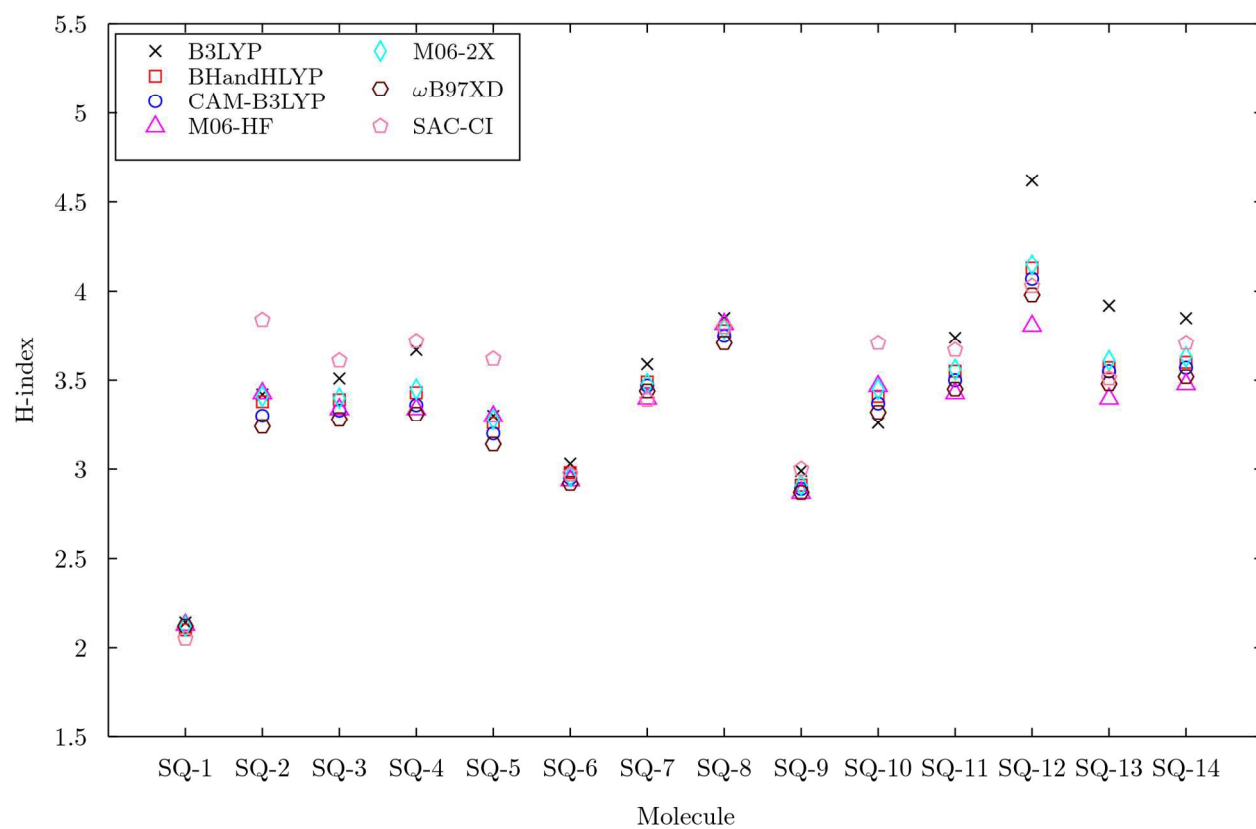
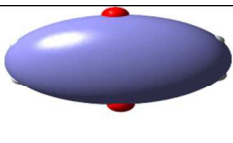
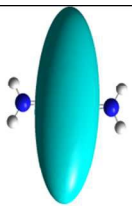
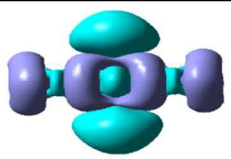
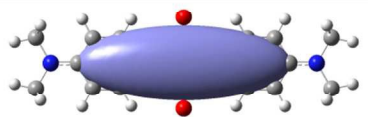
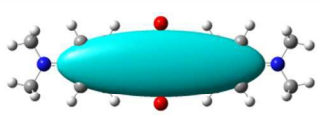
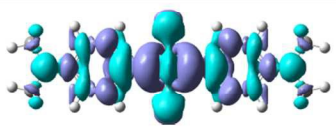
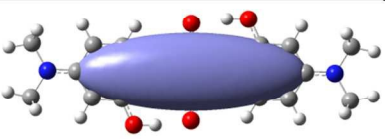
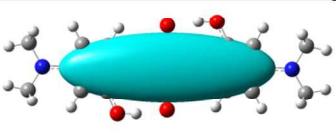
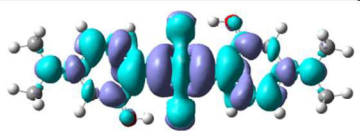
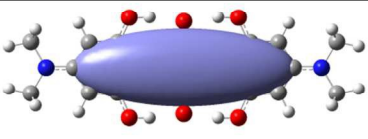
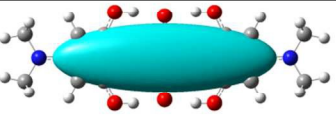
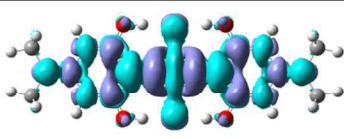
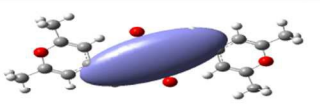
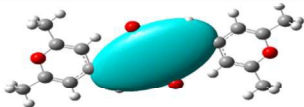
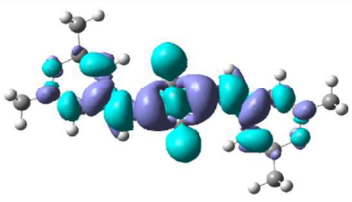
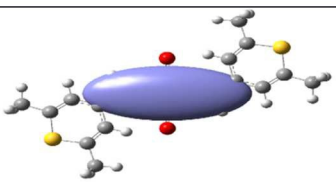
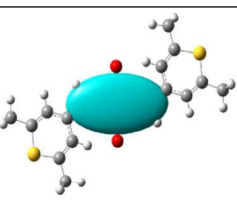
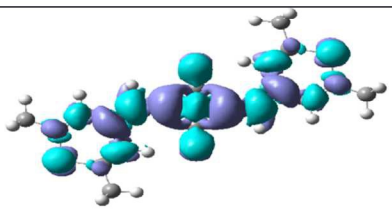


Figure 3: Centroids of charge increment ( $C^+$ ) and charge depletion ( $C^-$ ) and computed charge density difference ( $\Delta\rho$ ) between ground and excited states for SQ derivatives obtained at SAC/SAC-CI level (isosurface value = 0.0004).

Molecule	$C^+$	$C^-$	$\Delta\rho$
SQ-1			
SQ-2			
SQ-3			
SQ-4			
SQ-5			
SQ-6			
SQ-7	